Journal of Geophysical Research

Supporting Information for

Evidence of solid Earth influence on stability of the marine-terminating Puget Lobe of the Cordilleran Ice Sheet

Marion A. McKenzie[1*], Lauren E. Miller[1], Allison P. Lepp[1], and Regina DeWitt[2]

[1]Department of Environmental Sciences, University of Virginia, 291 McCormick Rd., Charlottesville, VA, USA 22904
[2]Department of Physics, East Carolina University, 1000 E. 5th St., Greenville, NC, USA 27858-4353

Corresponding author: Marion McKenzie (marion.mckenzie@mines.edu)

[*]Author now affiliated with the Geology and Geological Engineering Department, Colorado School of Mines, 1105 Illinois St., Golden, CO, USA 80201

Contents of this file

Introduction

The contents here within contain additional text on historic studies of Puget Lowland outcrop units (Text S1) and sample collection, preparation, and age determination of optically stimulated luminescence samples (Text S2). The results of the OSL data are less reliable than those of the radiocarbon dates. We lack nuclide information for adjacent layers of OSL taken on unit boundaries and faced feldspar contamination in samples. While there is some partial disagreement between radiocarbon and OSL dates, the OSL dates are still highly useful in providing approximate rates of landscape evolution based on bracketed ages of landscape emergence and submergence (Figure 2).

Figure S1 exemplifies the difference between lenses and laminations identified in the field. Figure S2 depicts a schematic of glacial retreat within a marine environment versus glacial retreat within a subaerial environment.

Table S1 is a compilation of site information and sample types collected. Table S2 is the OSL measurement sequence used for age determination.

Text S1. Over the last six decades, this region has been studied with multiple approaches, varying resolutions, and differing classification methods. Therefore, to provide continuity between our analysis and prior work on final glacial-ice occupation and post-glacial landscape evolution in the Puget Lowland, we provide a summary of stratigraphic units thought to record pre-LGM, LGM, and post-LGM deglaciation and landscape evolution.

S1.1 Pre-LGM and LGM deposits

A characteristic pre-LGM deposit in the Puget Lowland is the Lawton Clay, formed as the more southern Puget Lowland became a proglacial lake basin from ice advancement into the

northern Strait of Juan de Fuca (Mullineaux et al., 1965; Figure 1B). Southward migrating proglacial channels that were active 18,000-20,000 years ago formed extensive outwash plain deposits referred to as the Esperance Sands and mark the oncoming advance of the CIS in the Puget Lowland (Mullineaux et al., 1965; Crandell et al., 1966; Easterbrook, 1969; Clague, 1976; Booth, 1994). The final stage of ice sheet advance during late-stage MIS 2 in the Puget Lobe is known as the Fraser glaciation and is marked by the deposition of the massive diamicton called the Vashon Till (Willis, 1898; Easterbrook, 1969; Clague, 1981; Domack, 1983; Easterbrook, 1986). Previously radiocarbon dated-wood collected beneath the Vashon Till provides a maximum age for the timing of final ice advance to the latitude of around Seattle (47.608013°N) at ~14,500 ^{14}C years BP (~17,500 calendar years BP; Mullineaux et al., 1965; Porter & Swanson, 1998), although timing of maximum ice extent near Olympia, Washington (47.037872°N) is unknown and the degree of subglacial reworking and erosion of underlying strata is not well understood.

S1.2 Deglacial and post-glacial deposits

Overlaying the Vashon Till in some locations in the Puget Lowland is the shell-bearing Everson Glaciomarine Drift deposits (Armstrong et al., 1965; Easterbrook, 1969; Powell, 1980; Thorson, 1980; Pessl et al., 1981; Domack, 1983, 1984; Dethier et al., 1995), marking the Puget Lobe as primarily grounded below sea level (Thorson, 1980; Dethier et al., 1995; Demet et al., 2019). The oldest marine shells dated from the Everson Glaciomarine Drift suggest the Puget Lowland was deglaciated and open to marine influence by 13,500 ^{14}C years BP (~16,500 calendar years BP; Easterbook, 1992; Dethier et al., 1995; Swanson & Caffee, 2001). The lack of both sufficiently documented stratigraphic context for individual ages and a lack of marine reservoir correction for this region, however, contribute to uncertainties in this generalized date of deglaciation in the Puget Lowland (c.f., Porter & Swanson, 1998). Additionally, conflicting ages from freshwater lacustrine organics on the eastern fringe of the Puget Lowland suggest ice retreat before ~13,600 ^{14}C years BP (~16,500 calendar years BP; Rigg & Gould, 1957; Leopold et al., 1982; Anundsen et al., 1994), and numerous cosmogenic exposure ages consistently indicate that retreat occurred ~15,500 years ago (Swanson & Caffee, 2001), while much of the CIS also experienced Pleistocene Termination mass loss before significant climate reversals (Menounos et al., 2017).

The presence of the Everson Glaciomarine Drift has been used to suggest a marine incursion beneath the Puget Lobe (Dethier et al., 1995; Swanson & Caffee, 2001), inciting a rapid lift-off of grounded ice (i.e., rapid transition from grounded ice to a floating ice shelf) of the southernmost CIS (Thorson, 1980, 1981; Waitt & Thorson, 1983; Booth, 1987; Booth et al., 2003). Synchronous retreat of the Puget Lobe and the largely westward flowing Juan de Fuca Lobe due to the decoupling of the Puget Lobe from its bed due to marine incursion has also been suggested (Easterbrook, 1992). However, major differences in deglacial stratigraphy across the Puget Lowland (Powell, 1980; Pessl et al., 1981; Domack, 1984; Demet et al., 2019), indicate variable patterns of retreat in time and space. Additionally, modern elevation of marine limits in the Puget Lowland, range from ~125 m above sea level in the northern San Juan islands to less than 30 m at the southern end of Whidbey Island (Thorson, 1981, 1989; Dethier et al., 1995; Kovanen & Slaymaker, 2004; Polenz et al., 2005), which indicates highly variable rates of GIA across the region. Emergence of this landscape from below to above sea level is distinctly marked

in post-glacial stratigraphy by thin subaerial deposits (e.g., fluvial sediments and soil) overlying the glacial and glaciomarine deposits (Domack, 1984; Demet et al., 2019).

Text S2. Detailed text outlining OSL sample collection, processing, and age determination.

S2.1 Sample collection and preparation

Sediment samples were collected across unit boundaries with coarse-grain quartz material. In order to avoid pre-mature bleaching OSL, samples were collected before sunrise or after sunset, were only exposed to low energy red light, and were wrapped in opaque black plastic before being transported to East Carolina University (ECU) for preparation and processing. Sample preparation was carried out under dark-room conditions using standard coarse-grain procedures: samples were wet-sieved at 90-125 μm with some expansion to grain sizes of 63-212 μm. After drying the samples at 50 °C, the samples were treated with 10 % hydrochloric acid (HCl) and 29 % hydrogen peroxide (H_2O_2). A high-density separation was conducted with lithium heteropolytungstate (LST) at a density of 2.72-2.75 g/cm^3 to isolate quartz grains. Coarse grains were etched for 40 minutes with 48% hydrofluoric acid (HF) to remove outer parts affected by alpha radiation, followed by a 10% HCl rinse to remove fluoride precipitates. A low-density separation to isolate quartz from feldspar was conducted with LST at a density of 2.62 g/cm^3. After final sieving, the aliquots were prepared by using Reusch Silkospray to adhere material to the stainless steel sample cups.

Bulk sediment was collected from outcrops for gamma spectrometry measurements and stored for at least 4 weeks prior to measurement. While the OSL samples were taken at unit boundaries, the dose rate samples were taken from the same unit as the OSL samples. Therefore, the gamma dose rates reflect the sample unit only and contain no information about adjacent, underlying, or overlying units.

S2.2 Age determination

Dose measurements were conducted using a Risø TL/OSL-DA-20 reader manufactured by Risø National Laboratory with a bialkali PM tube (Thorn EMI 9635QB). The built-in ^{90}Sr/^{90}Y beta source gives a dose rate of ~100 mGy/s. Optical stimulation was carried out with an IR LED array at 870 nm with 121 mW/cm^2 (90 %) power at the sample, a blue LED array at 470 nm with 74 mW/cm^2 (90 %) power at the sample and a 7.5 mm Hoya U-340 detection filter (290-370 nm; Bøtter-Jensen & Murray, 1999). Equivalent doses were determined following the single-aliquot regenerative dose (SAR) procedure developed by Murray and Wintle (2000) and Wintle and Murray (2006). Due to feldspar contamination, a post-IR procedure was used to isolate quartz signals in the equivalent dose measurements (Wallinga et al., 2002). The preheat temperature of 180 °C for 10 s was determined for each sample using plateau and dose recovery tests. Our specific measurement protocol is outlined in Table 2. Luminescence signals L_i and T_i were determined by integrating over the first 0.8 seconds of an OSL decay curve and subtracting an average of the next 4 seconds as background signal. The signal uncertainty followed from counting statistics. The sensitivity corrected signal is given by $C_i = L_i/T_i$. The dose response of every aliquot was determined by fitting the luminescence signals C_1 to C_5 with a saturating exponential. The dose D_0 corresponding to the natural sensitivity-corrected luminescence signal C_0, was calculated with the fitting parameters. All uncertainties were calculated using the Gaussian law of error propagation and Poisson statistics. The vast majority of aliquots passed the reliability test – requiring recycling ratios between 0.9 and 1.1, dose recovery <10 % deviation from given dose, low recuperation. The equivalent dose D_e was determined for each site using the central age model (Galbraith, 1999). The full uncertainty also includes 3.1 % for the built-in beta source error.

In the sediment, grains are exposed to natural gamma and beta radiation from uranium, ^{232}Th, and potassium. The concentrations of these radionuclides were measured with high

resolution gamma spectrometry. Uranium concentrations determined from ^{234}Th were all significantly higher than concentrations determined from ^{214}Pb and ^{214}Bi. We assumed that ^{234}U was leached out of the sample due to in situ water presence.

Dose rates were calculated by using the actual measured concentrations for the nuclides in the uranium decay chain. Uncertainties were calculated based on the maximum and minimum values obtained from the measured concentrations of ^{234}Th and ^{214}Bi/^{214}Pb. Water contents were very low and have an uncertainty of 5 % (Table 2). Beta and gamma dose rates were calculated using the conversion factors published by Guérin et al. (2011). The cosmic dose rate was calculated as described by Prescott and Stephan (1982), Barbouti and Rastin (1983), and Prescott and Hutton (1994) and incorporates site latitude, longitude, site altitude, and sample depth below surface. The effective thickness was assumed to be half the burial depth with uncertainty of 5 %.

The sample ages, calculated in calendar years, were calculated by dividing the dose by the dose-rate (Table 2). Due to feldspar contamination in some samples, fading was measured with a post-IR blue sequence for all samples. Only some of the samples showed fading. For those, the ages were corrected as suggested by Auclair et al. (2003). While ^{14}C ages are reported in kilo years ago (kya) calendar year BP (1955), all OSL ages are reported in kya based on the date of collection (2020). OSL ages in kya can be directly compared to kya cal. BP by subtracting 72 years from the OSL age.

Figure S1. A clay lamination seen in Unit 3 of Fort Casey Site 1 (left) and a silt lens seen in Unit 1 of Fort Casey Site 1 (right). This distinction is maintained throughout all site stratigraphic descriptions.

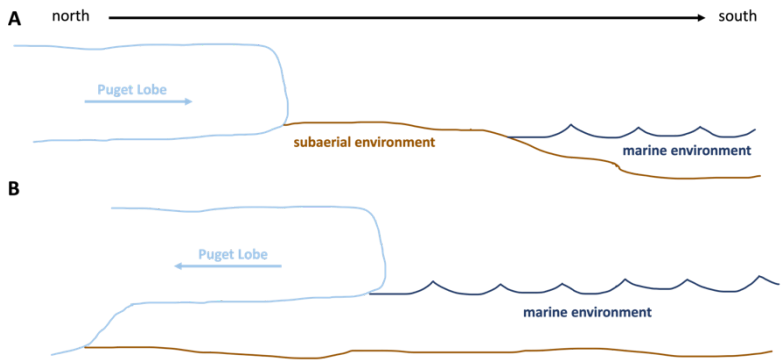

Figure S2. Schematic drawing of A) time 1 indicating Puget Lobe advance into subaerial Puget Lowland post landscape emergence (Figure 2). B) Indicates time 2 Puget Lobe ice retreat within a

marine environment post landscape-submergence and marine-incursion following time 1. Puget Lobe ice retreat in a marine environment only occurred at southernmost sites Double Bluff and Penn Cove (Figure 2).

Table S1. Site and sample collection information.

Site	Sediment samples	Radiocarbon samples	OSL samples
Double Bluff (a)	53	2	0
Fort Casey (b)	20	0	2
Penn Cove (c)	126	8	2
West Beach (d)	54	4	6
Cliffside (e)	29	0	0
Total	**282**	**14**	**12**

Table S2. OSL measurement sequence

1. Radiation dose D_i
2. Preheat at 180°C* for 10s
3. IRSL at 125°C for 150s to remove feldspar signal
4. OSL at 125°C for 100s, measure OSL signal L_i
5. Fixed test radiation dose D_t**
6. Cutheat at 160°C to remove unstable signals
7. IRSL at 125°C for 150s to remove feldspar signal
8. OSL at 125°C for 100s, measure OSL signal T_i
9. Repeat steps 2-8 for cycle 0 and steps 1-8 for cycles 1-7

Cycle 0: Natural signal, $D_0 = 0$ Gy with no administered dose
Cycle 1-5: Regenerative doses, D_1, $D_2<D_1<D_3<D_0<D_4<D_5$
Cycle 6: Dose recovery test, $D_6=D_4$***
Cycle 7: Recycle test, $D_7=D_1$***
Cycle 8: Recuperation test, $D_8=0$

* preheat temperature determined by plateau test
** D_t= 15-20% D_0

*** administered to check the precision with which a known dose can be recovered